ChemComm

Accepted Manuscript

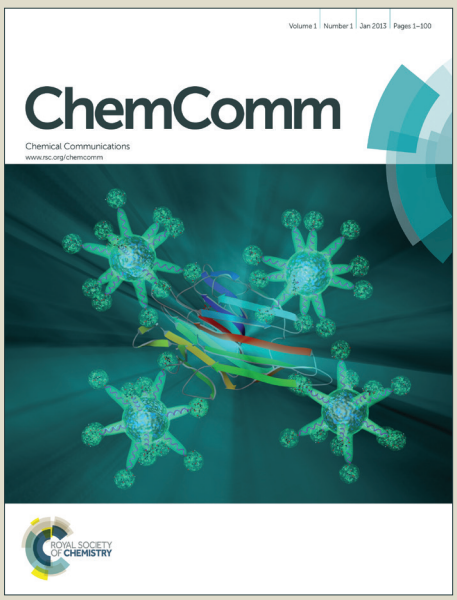

ROYAL SOCIETY OF CHEMISTRY

www.rsc.org/chemcomm

Cite this: DOI: 10.1039/c0xx00000x

www.rsc.org/xxxxxx

ARTICLE TYPE

A Two-Ring Interlocked DNA Catenane Rotor Undergoing Switchable Transitions Across Three States†

Xiu-Juan Qi,[a,b‡] Chun-Hua Lu,[b‡] Alessandro Cecconello,[b] Huang-Hao Yang,[a] and Itamar Willner*[b]

Received (in XXX, XXX) Xth XXXXXXXXX 20XX, Accepted Xth XXXXXXXXX 20XX

DOI: 10.1039/b000000x

A two-ring (α/β) interlocked DNA catenane rotor system is described. Using appropriate fuel and anti-fuel strands, the triggered switchable rotation across three states S_1, S_2 and S_3 associated with the circular track of ring α is demonstrated.

The synthesis of DNA machines, such as tweezers,[1] walkers[2] or cranes,[3] attracted recent research efforts, and such molecular devices were implemented for controlled synthesis,[4] carrying of nanoscale cargoes,[5] and switchable plasmonic phenomena.[6] Different external stimuli, such as pH,[7] metal ions,[8] light[9] or nucleic acids[1] were used as fuels to stimulate the DNA machines. Similarly, different readout signals such as fluorescence,[10] electrical or photoelectrochemical outputs[11] were applied to image the mechanical transitions of the DNA molecular devices. Among the DNA machines, interlocked DNA rings find recent interest.[12] DNA catenanes appear in nature,[13] and synthetic methods for the preparation of artificial interlocked DNA rings were developed and their structures were imaged at the single-molecule level.[14,15]

Recently DNA catenanes undergoing programmed switchable transitions across defined states were characterized.[15] For example, a three-ring catenane structure undergoing programmed transitions across three states was prepared. The switchable mechanical transitions of the system were used to organize switchable structures of Au nanoparticle assemblies and to control the fluorescence properties of a fluorophore by means of a Au nanoparticle tethered to the DNA scaffold.[16] Similarly, a two-ring interlocked catenane system was reported to act as rotary motor with controlled directionality upon triggering the system with Hg^{2+} ions/cysteine or pH (H^+/OH^-) as fuel and anti-fuel stimuli.[17] Finally, a two-ring catenane system acted as a pH-driven DNA pendulum upon subjecting the system to an oscillatory pH environment that drives the pendulum across two states by the pH-stimulated formation and dissociation of an i-motif structure.[18] In the present report we describe a two-ring catenane system that undergoes cyclic switchable transitions between three states using nucleic acid strands as fuels and anti-fuels. The switchable transitions are followed by fluorescence quenching of fluorophores, associated with the device, using a molecular quencher or a Au nanoparticle (NP) quencher tethered to the rotor DNA.

The stability of duplex nucleic acid structures is controlled by the number of base pairs and the nature of complementary bases (A-T or C-G).[19] The energetics of duplex DNAs has been implemented to reconfigurate DNA structures, and the energy-driven strand-displacement principle has been widely applied to construct DNA structures, to develop amplified sensing platforms, to develop DNA computing circuits, and to develop DNA machines.[20] For example, DNA tweezers, walkers or switches were developed by the strand displacement paradigm.[21] In the present study, we use this principle to stimulate the transitions of a DNA rotor in a two-ring catenane system.

The synthesis of the two-ring catenane α/β is schematically outlined in Fig. 1(A). The two strands L_α and L_β include complementary base-pair regions I and I'. The capping of the 3'- and 5'-ends of the interthreaded strands L_α and L_β with the strands C_α and C_β leads to the respective quasi-ring. The ligase-stimulated ligation of the quasi-rings, and the subsequent removal of the capping units by electrophoretic separation and extraction of the two ring catenane, led to the pure interlocked two-ring catenane. Fig. 1(B) depicts the electrophoretic separation of the mixture generated upon the synthesis of the interlocked α/β catenane and of the components used to construct the interlocked structure. Lanes (1) and (3) show the bands corresponding to the linear strands L_β and L_α, respectively, while lanes (2) and (4) depict the bands corresponding to the single rings prepared by capping and ligation of L_β and L_α, respectively. In lane (5) are shown the bands formed upon ligation of the strands L_α and L_β in the presence of C_α and C_β, according to Fig. 1(A). In addition to the bands corresponding to single rings α and β (formed by kissing interactions between L_α and L_β followed by ligation), a high molecular weight structure corresponding to the inter-threaded catenane consisting of the two rings α and β is observed. Extraction of the band corresponding to the α/β catenane yielded the pure interlocked structure, lane (6).

Fig. 2(A) depicts the design of the switchable three states rotor and the fuel/anti-fuel transitions of the rotor system. Ring α was designed to include three sites I, II and III that can bind to the sequence I' associated with ring β. Nonetheless, base mismatches are included in the sites II and III so that the duplex stabilities follow the order $E_{I'/I} > E_{I'/II} > E_{I'/III}$. Ring α is internally modified with the fluorophores Cy3 and Cy5 at the marked positions. The ring β is modified by an auxiliary nucleic acid strand, (**1**), functionalized at its 3-end with the black hole quencher 2 (BHQ-2). The sequences F_2 and F_3 hybridize partially with the sequences associated with sites II and III, and partially to extended domains of these sites. The duplexes between F_2 and F_3

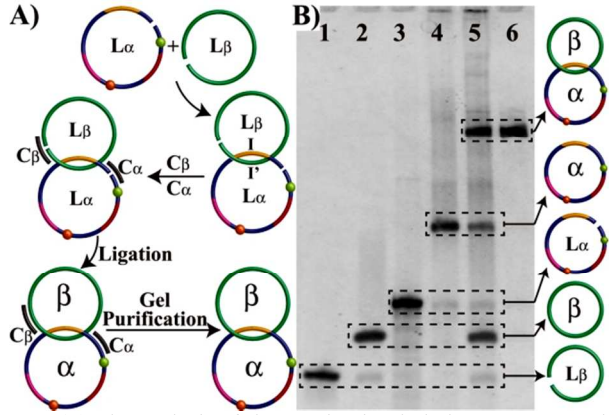

Fig. 1. (A) The synthesis of the two-ring interlocked DNA catenane that includes two internal fluorescence labels in ring α. (B) Gel electrophoresis characterization of the stepwise synthesis and purification of the two-ring catenane α/β. Lanes 1-4 bands corresponding to the individual components displayed on the right. Lane 5 – bands corresponding to the final mixture obtained upon synthesis of the α/β two-ring catenane. Lane 6 – gel electrophoretic purified α/β two-ring catenane.

with the ring α are energetically stable resulting in the formation of state S_1 where ring β is positioned on site I. Treatment of state S_1 with the strand F_1 and aF_2 results in the displacement of ring β from the site I and the displacement of F_2 through the formation of the energetically-favored duplex F_2/aF_2. Therefore, the released ring β and the vacant hybridization site II on ring α stimulate the hybridization of ring β with site II, and the formation of state S_2. Further treatment of state S_2 with F_2 and aF_3 displaces ring β from site II and displaces the strand F_3 from site III, processes that stimulate the transition of ring β to site III leading to the formation of state S_3. The subsequent treatment of state S_3 with F_3 and aF_1 leads to the strand displacement of ring β from site III and of the F_1 strand associated with site I, resulting in the recovery of state S_1.

The rotor direction can also be triggered in the anti-clockwise direction $S_1 \rightarrow S_3 \rightarrow S_2 \rightarrow S_1$ by applying the appropriate displacement strands. Previous studies have demonstrated that transitions of the rotor proceed along the shortest paths and that duplex nucleic acids introduce barriers for rotation and dictate transitions across single stranded paths,[17] the clockwise and anti-clockwise rotations of ring β in the presence of the appropriate strands is supported. The transitions across the states could then be probed by following the fluorescence intensities of the two fluorophore markers associated with ring α (Cy3 and Cy5). In state S_1 the two fluorophores are spatially separated from the quencher unit, giving rise to higher fluorescence of the two fluorophores. The fluorescence intensities of the fluorophore in state S_1 provide the reference intensities for the transitions of the rotor. The transition of state S_1 to state S_2 results in the effective quenching of the fluorescence of Cy3, due to the proximity between the fluorophore and the quencher. The fluorescence of Cy5 in State S2 is, however, almost unaffected due to the spatial separation between Cy5 and the quencher. The transition of the rotor from state S_2 to state S_3 leads to close proximity between the quencher and the fluorophore Cy5, while the Cy3 fluorophore is spatially separated from the quencher. This leads in state S_3 to low fluorescence of Cy5 and high fluorescence of Cy3. Similarly, the anti-clockwise rotation of the rotor across the states $S_1 \rightarrow S_3 \rightarrow S_2 \rightarrow S_1$ can be followed by the fluorescence intensities of the

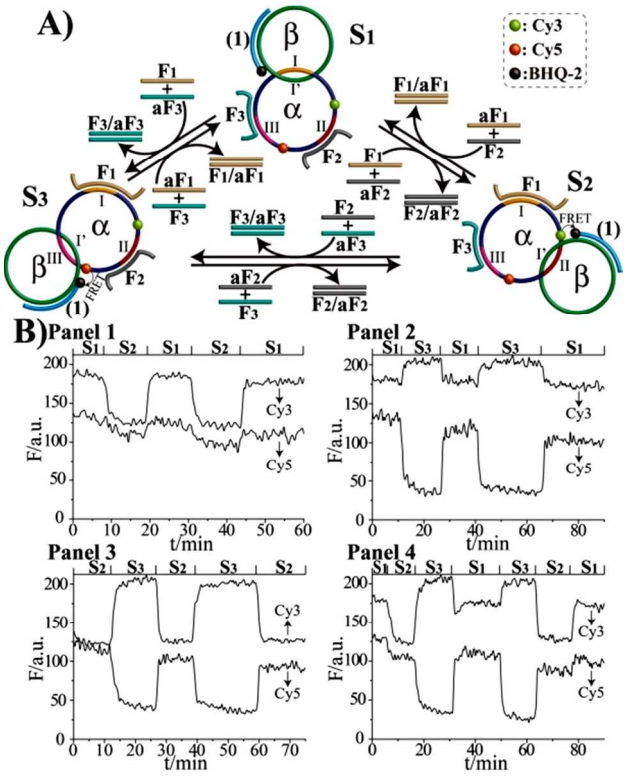

Fig. 2. (A) Switchable transitions of the two-ring catenane between the states S_1, S_2 and S_3 upon the application of the respective fuel and anti-fuel strands and following the transitions by the quenching of the internal fluorophores by a quencher with hybridized with the moving ring β. (B) Time-dependent fluorescence changes of the internal fluorescence labels Cy3 and Cy5 upon: Panel 1 – The switchable and reversible transitions between S_1 and S_2. Panel 2 – The switchable and reversible transitions between S_1 and S_3. Panel 3 – The switchable and reversible transitions between S_2 and S_3. Panel 4 – The cyclic switchable transitions $S_1 \rightarrow S_2 \rightarrow S_3 \rightarrow S_1 \rightarrow S_3 \rightarrow S_2 \rightarrow S_1$.

two probes. Fig. 2(B) depicts the cyclic fluorescence intensities of the two fluorophores upon the cyclic and reversible transitions of the ring β across the different states. In panel 1, the fluorescence changes upon the reversible transitions between S_1 and S_2 are examined. The formation of state S_2 is accompanied by the fluorescence quenching of Cy3 and a little fluorescence change of Cy5. The reversible switchable transitions between S_1 and S_3 are depicted in panel 2 showing that the fluorescence of Cy3 is almost unaffected while the fluorescence of Cy5 is quenched. In Fig. 2(B) panel 3, the fluorescence changes upon the reversible transitions between S_2 and S_3 are displayed. The formation of S_3 is accompanied with a fluorescence increase of Cy3 and the concomitant fluorescence decrease of Cy5. The reverse transition of S_3 to S_2 is reflected by the opposite fluorescence increase of Cy5 and fluorescence quenching of Cy3. Finally, Fig. 2(B), panel 4 shows the fluorescence changes upon the cyclic transitions $S_1 \rightarrow S_2 \rightarrow S_3 \rightarrow S_1 \rightarrow S_3 \rightarrow S_2 \rightarrow S_1$. As expected, the transition of S_1 to S_2 leads to the quenching of Cy3 and the subsequent transition to S_3 results in the quenching of Cy5. The recovery of state S_1 regenerates the reference fluorescence intensities of the two fluorophores. The counter rotation of the rotor ring leads, as expected, to the opposite fluorescence changes.

The stepwise transitions of the rotor were similarly probed by using a Au NP as quencher of the fluorophore probes, Fig. 3(A). Toward this end, 10 nm-sized Au NPs were functionalized with a

single nucleic acid (**2**). (For the synthetic details on the preparation of the (**2**)-modified Au NPs see supporting information). The (**2**)-modified Au NPs were hybridized with domain "x" of ring β. The switchable and reversible transitions of the rotor across the states S_1, S_2 and S_3 upon subjecting the system to the respective strands are schematically presented in Fig. 3(A). The fluorescence changes accompanying the cyclic and reversible rotation of ring β across the states are depicted in Fig. 3(B). The transition of ring β from state S_1 to S_2 is accompanied by the quenching of Cy3 and a less effective quenching of Cy5. The opposite transition of state S_1 to S_3 results in the quenching of Cy5, while the fluorescence of Cy3 is less efficient. By the reverse transitions of S_2 to S_1 or S_3 to S_1 the reference fluorescence intensities of the spatially separated fluorophores from the Au NP are regenerated. Fig. 3(B), shows the sequential fluorescence changes upon the stepwise transitions of the rotor β across the states $S_1 \rightarrow S_2 \rightarrow S_3 \rightarrow S_1$ and the reverse transitions $S_1 \rightarrow S_3 \rightarrow S_2 \rightarrow S_1$. Evidently, the clockwise rotation is accompanied upon formation of S_2 with the fluorescence quenching of Cy3, upon formation of S_3 the quenching of the fluorescence of Cy5, and upon regeneration of S_1 the reference fluorescence of the device. Similarly, the anti-clockwise rotation process leads in the first step, generating S_3, to the quenching of the fluorescence of Cy5 to the subsequent fluorescence quenching upon forming Cy3, upon forming S_2, and to the regeneration of the reference fluorescence intensities of Cy3 and Cy5 corresponding to the S_1 state. The present study has demonstrated that the reconfiguration of the state S_1 into the states S_2 or S_3 leads to the quenching of the fluorophores Cy3 and/or Cy5 by the Au NPs, respectively. Recent studies have revealed, however, that by appropriate tuning of the distances between the fluorophore and the Au NPs the reconfiguration of the structures might lead either to surface enhanced fluorescence or fluorescence quenching phenomena.[6,16] Thus, by further tuning the sizes of the Au NPs and the distances separating the fluorophore/Au NPs on the rotor device, interesting plasmonic phenomena may be envisaged.

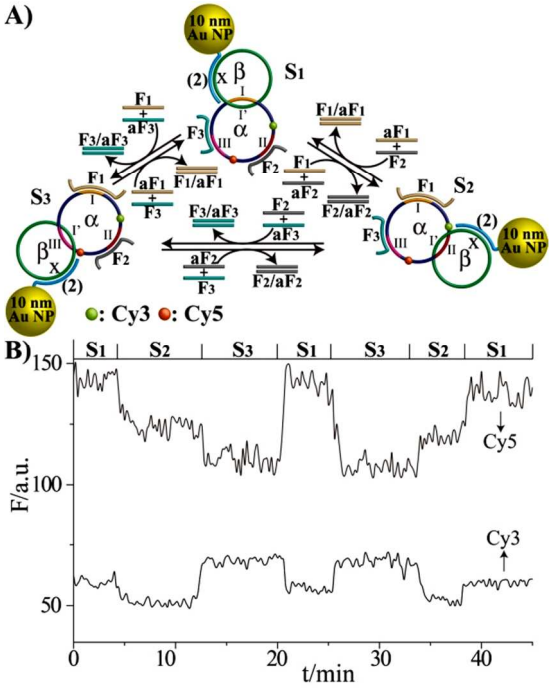

Fig. 3. (A) Following the switchable transitions of the two-ring catenane across states S_1, S_2 and S_3 by the quenching of the internal fluorophores by a Au NPs tethered to the moving ring β. (B) Time-dependent fluorescence changes upon the cyclic and reversible transitions across the states: $S_1 \rightarrow S_2 \rightarrow S_3 \rightarrow S_1 \rightarrow S_3 \rightarrow S_2 \rightarrow S_1$.

In conclusion, the present study has described an interlocked two-ring catenane rotor system driven by strand-displacement processes across three states. The internal modification of one of the rings (ring α) with two fluorophore units enabled us to probe the stepwise transitions of the rotor across the states using the spatially-controlled interactions between an auxiliary molecular quencher or a Au NP with the different fluorophores. Such dictated reconfiguration processes across pre-designed state demonstrate the assembly of a simple finite-state machine. By increasing the number of interlocked rings, finite-state machines of enhanced complexities may be envisioned. Furthermore, the circular structure of the catenane system lacking 3'- or 5'-ends, suggests that these structures would reveal stability against enzymatic digestion. Thus, the catenanes could act as carrier for intracellular applications, and the reconfiguration of the motor device could release DNA strands that affect intracellular processes and signal pathways.

This research is supported by the FET open EU program, MULTI project.

Notes and references

[a] *The Key Lab of Analysis and Detection Technology for Food Safety of the MOE, College of Chemistry and Chemical Engineering, Fuzhou University, Fuzhou 350002, China*
[b] *Institute of Chemistry and Center for Nanoscience and Nanotechnology, The Hebrew University of Jerusalem, Jerusalem 91904, Israel*
E-mail: willnea@vms.huji.ac.il

† Electronic Supplementary Information (ESI) available: DNA sequences, synthesis of two-ring catanene, synthesis of single nucleic acid-modified Au NPs. See DOI: 10.1039/b000000x/

‡ These authors contributed equally to this work.

1 B. Yurke, A. J. Turberfield, A. P. Mills Jr., F. C. Simmel and J. L. Neumann, Nature, 2000, **406**, 605.
2 (a) J. S. Shin and N. A. Pierce, *J. Am. Chem. Soc.*, 2004, **126**, 10834; (b) T. Omabegho, R. Sha and N. C. Seeman, *Science*, 2009, **324**, 67; (c) C. Wang, J. Ren and X. Qu, *Chem. Commun.*, 2010, **47**, 1428.
3 Z. G. Wang, J. Elbaz and I. Willner, *Angew. Chem., Int. Ed.*, 2012, **51**, 4322.
4 (a) P. J. Milnes, M. L. McKee, J. Bath, L. Song, E. Stulz, A. J. Turberfield and R. K. O'Reilly, *Chem. Commun.*, 2012, **48**, 5614; (b) M. L. McKee, P. J. Milnes, J. E. Stulz, R. K. O'Reilly and A. J. Turberfield, *J. Am. Chem. Soc.*, 2012, **134**, 1446.
5 (a) S. M. Douglas, I.Bachelet and G. M.Church, *Science,* 2012, **335**, 831; (b) J. Elbaz and I. Willner, *Nat. Mater.*, 2012, **11**, 276.
6 S. Shimron, A. Cecconello, C. H. Lu and I. Willner, *Nano Lett.*, 2013, **13**, 3791.
7 J. Elbaz, Z. G. Wang, R. Orbach and I. Willner, *Nano Lett.*, 2009, **9**, 4510.
8 Z. G. Wang, J. Elbaz, F. Remacle, R. D. Levine and I. Willner, *Proc. Natl. Acad. Sci. U.S.A.*, 2010, **107**, 21996.
9 (a) X. Liang, H. Nishioka, N. Takenaka and H. Asanuma, *Chembiochem*, 2008, **9**, 702; (b) M. You, F. Huang, Z. Chen, R. W. Wang and W. Tan, *ACS Nano,* 2012, **6**, 7935
10 Z. G. Wang, J. Elbaz and I. Willner, *Nano Lett.*, 2010, *11*, 304.
11 X. Liu, A. Niazov-Elkan, F. Wang and I. Willner, *Nano Lett.*, 2013, **13**, 219.
12 (a) D. Ackermann, T. L. Schmidt, J. S. Hannam, C. S. Purohit, A. Heckel and M. Famulok, *Nat. Nanotechnol.*, 2010, **5**, 436; (b) D. Han, S. Pal, Y. Liu and H. Yan, *Nat. Nanotechnol.,* 2010, **5**, 712; (c) T. L. Schmidt and A. Heckel, *Nano Lett.,* 2011, **11**, 1739.

13 B. Hudson and J. Vinograd, *Nature*, 1967, **216**, 647.
14 Y. Liu, A. Kuzuya, R. Sha, J. Guillaume, R. Wang, J. W. Canary and N. C. Seeman, *J. Am. Chem. Soc.*, 2008, **130**, 10882.
15 J. Elbaz, Z. G. Wang, F. Wang and I. Willner, *Angew. Chem., Int. Ed.*, 2012, **51**, 2349.
16 J. Elbaz, A. Cecconello, Z. Fan, A. O. Govorov and I. Willner, *Nat. Commun.*, 2013, **4**, 2000.
17 C. H. Lu, A. Cecconello, J. Elbaz, A. Credi and I. Willner, *Nano Lett.*, 2013, **13**, 2303.
18. X. J. Qi, C. H. Lu, X. Liu, S. Shimron, H. H. Yang and I. Willner, *Nano Lett.*, 2013, **13**, 4920.
19 D. Y. Zhang and G. Seelig, *Nat. Chem.*, 2011, **3**, 103.
20 (a) Y. Tian and C. Mao, *J. Am. Chem. Soc.*, 2004, **126**, 11410; (b) S. Venkataraman, R. M. Dirks, P. W. Rothemund, E. Winfree and N. A. Pierce, *Nat. Nanotechnol.*, 2007, **2**, 490; (c) F. Wang, J. Elbaz, R. Orbach, N. Magen and I. Willner, *J. Am. Chem. Soc.*, 2011, 133, 17149; (d) L. Qian and E. Winfree, *Science*, 2011, **332**, 1196; (e) L. Qian, E. Winfree and J. Bruck, *Nature*, 2011, **475**, 368; (f) G. Pelossof, R. Tel-Vered, X. Liu and I. Willner, *Nanoscale*, 2013, **5**, 8977.
21 (a) Y. Tian, Y. He, Y. Chen, P. Yin and C. Mao, *Angew. Chem., Int. Ed.*, 2005, **44**, 4355; (b) J. Bath, S. J. Green and A. J. Turberfield, Angew. Chem., Int. Ed., 2005, **44**, 4358; (c) T. Omabegho, R. Sha and N. C. Seeman, Science, 2009, **324**, 67; (d) S. F. Wickham, M. Endo, Y. Katsuda, K. Hidaka, J. Bath, H. Sugiyama and A. J. Turberfield, *Nat. Nanotechnol.*, 2011, **6**, 166; (e) L. Xin, C. Zhou, Z. Yang and D. Liu, Small. 2013, 9, 3088; (f) M. Liu, J. Fu, C. Hejesen, Y. Yang, N. W. Woodbury, K. Gothelf, Y. Liu and H. Yan, *Nat. Commun.*, 2013, **4**, 2127.